

Ordering and multiple phase transitions in ultra-thin nickelate superlattices

Danilo Puggioni, Alessio Filippetti, and Vincenzo Fiorentini

*Dipartimento di Fisica dell'Università di Cagliari and CNR-IOM, UOS Cagliari,
Cittadella Universitaria, I-09042 Monserrato (CA), Italy*

(Dated: July 12, 2022)

We interpret via advanced ab initio calculations the multiple phase transitions observed recently in ultra-thin $\text{LaNiO}_3/\text{LaAlO}_3$ superlattices. The ground state is insulating, charge-ordered, and antiferromagnetic due to concurrent structural distortion and weak valency disproportionation. We infer distinct transitions at 40 K and 150 K, respectively, from antiferromagnetic order to moment disorder, and from structurally-dimerized insulator to an undistorted metallic Pauli paramagnet (exhibiting a cuprate-like Fermi surface). The results are in satisfactory agreement with experiment.

PACS numbers: 71.30.+h,75.25.Dk,75.70.-i

Correlated materials are often characterized by incipient or actual instabilities towards collective ordered states. Recent experiments [1, 2] have investigated, via an elegant nanostructuring manipulation of materials properties, the phase transitions playing out in LaNiO_3 (LNO henceforth – in the bulk the only metallic Pauli-paramagnetic (PM) rare-earth nickelate) in an intentionally perturbed environment, namely epitaxially-strained ultra-thin superlattice (SL) of alternating layers of LNO and of the band insulator LaAlO_3 (LAO). For sufficiently thin LNO (2-3 layers at most), nearly concurrent multiple transitions from a non-magnetic normal metal to a long-range-ordered magnetic, insulating, charge-ordered state were revealed by a crossover in conductivity temperature (T) dependence, muon spin rotation (μSR), spectral weight transfer in optical conductivity [1], and XAS (x-ray absorption spectroscopy) line splitting [2]. Magnetometry (measuring zero total magnetization) and μSR rotation (detecting magnetic moments with a lower-bound value $0.5 \mu_B$ and line shape compatible with long-range order) strongly support long-range antiferromagnetic (AF) order [1].

The precise nature of the low- T state of the LNO/LAO SL and the transitions it undergoes is unclear. Here we address the problem from first principles studying a strained ultra-thin LNO/LAO SL using variational self-interaction-corrected local density functional theory (VPSIC) [3, 4], a parameter-free method which provides an improved description of many correlated and magnetic materials compared to semi-local approaches. So far, ab initio calculations have neither been able to identify an AF ground state as observed for these SLs, nor, a fortiori, to provide a general picture of the rich experimental situation. Local (LDA) or gradient-corrected (GGA) density functionals find neither a stable AF phase nor distorted structures, even starting from dimerized and polarized initial conditions, as we verified explicitly. LDA/GGA+U predicts ferromagnetic ground states not seen in experiment, apparently irrespective of U [5]. The satisfactory agreement of VPSIC with experiment demonstrated below suggests an improved account for

on-site correlations, also indicated by points of agreement with dynamical mean field theory (DMFT) results for simplified geometries and magnetic states [6].

The ground state we find (labeled AFD henceforth) is structurally dimerized, charge-ordered, insulating, and antiferromagnetic with modulation vector $(0, \pi/2)$, in partial analogy with bulk rare-earth nickelates [9]. From the calculated energetics, we infer magnetic-ordering and metal-insulator transitions at two distinct critical temperatures of 40 and 150 K respectively. The transitions are driven by structural dimerization and partial valency disproportionation of Ni atoms at low T , inducing magnetic superexchange and Mott localization. In addition, we calculate the T -dependent SL conductivity within Bloch-Boltzmann theory [10] and discuss a possible concurrent metal-insulator-transition mechanism. The results are largely consistent with the data of Ref.1. Finally, we find that the high- T metallic Pauli-PM phase has a Fermi surface akin to optimally-doped cuprates, as foreseen in earlier theoretical work [7, 11], and that metastable phases could exhibit underdoped cuprate-like Fermi surfaces.

Method details – Total energy, force, and band structure calculations are performed by VPSIC [3] using the plane-wave ultrasoft pseudopotential method (energy cutoff 30 Ryd, $4 \times 4 \times 4$ k-mesh, smearing 20 mRyd for the metal phases) in the supercell approach. The epitaxially-strained LNO/LAO (1+1) SL are simulated at a tensile planar strain of about 3% as in typical experiments. The LNO layers contain up to four Ni atoms to simulate antiferromagnetic structures. We optimize the cell length, and atomic positions according to quantum forces [3]. The *dc* conductivity is calculated in Bloch-Boltzmann theory [10] with a relaxation time approximation using ab initio band energies on dense k grids (over 2000 points).

Structure and charge ordering – In the AFD ground state the nominally trivalent Ni_{III} atoms of LNO are inequivalent due to strong cooperative dimerization of the Ni-centered octahedra. All Ni-O bonds around each Ni either expand or contract from 2 Å to 2.19 Å or respectively 1.83 Å in a predominantly breathing mode. Calcu-

lated octahedra rotations are minor ($\sim 1\text{-}2^\circ$). The short and long bonds match those, respectively, in peroxonickel complexes with nominally tetravalent Ni_{IV} and NiO with nominally divalent Ni_{II} . (We adopt these labels below for convenience). The distortion is indeed accompanied by charge transfer from Ni_{IV} to Ni_{II} , which we quantify by VPSIC occupations [3]. The total transfer is 0.07 $|\text{e}|$, in fair agreement with 0.03 $|\text{e}|$ estimated [1] from the difference of integrated optical conductivity above and below the transition. This charge-ordered bond-dimerized phase is at least compatible with the splitting in the SL XAS spectra, analogous to insulating nickelates [2], although we cannot provide a quantitative estimate of that splitting from our calculation. The magnetic order and insulating character of this state tend to confirm this conclusion, as discussed below.

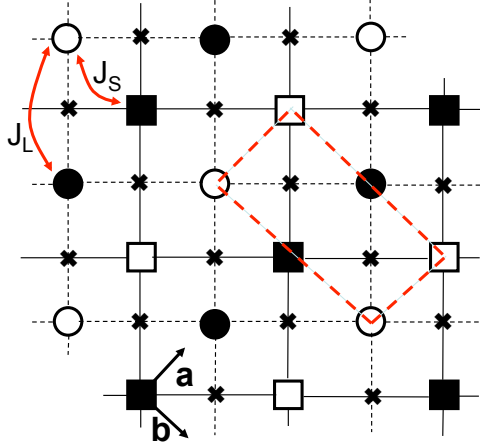


FIG. 1. (Color online) Magnetic order of the LNO/LAO (1+1) SL. Squares, circles: up (filled) and down (empty) polarized Ni_{II} ; crosses: unpolarized Ni_{IV} . Circles and squares indicate distinct interpenetrating cubic AF lattices (see text). Oxygens (not shown) sit on connecting lines roughly halfway between Ni's. The $2\sqrt{2}\times\sqrt{2}$ simulation cell is indicated (long-dash).

Magnetism – In the AFD state the structural and valency dimerization are associated with the pattern sketched in Fig.1. In our single-LNO-layer cell there is no vertical modulation by construction; the planar modulation $\mathbf{q}=(0,\pi/2)$ on the (reciprocal) \mathbf{a},\mathbf{b} basis, the same as in bulk monoxides [3], is analogous to insulating nickelates [9], with the difference that the “ $\text{Ni}(3-\delta)$ ” are polarized in those systems, but completely non-magnetic here. Indeed, Ni_{II} ’s [squares, circles in the Figure] carry a moment $\mu_{\text{Ni}_{\text{II}}}=\pm 1.44 \mu_B$, while Ni_{IV} ’s [crosses in the Figure] have zero moment, confirming a qualitative picture of Ni_{II} disproportionation into unpolarized Ni_{IV} $t_{2g}^6 e_g^0$ and polarized Ni_{IV} $t_{2g}^6 e_g^2$. Overall, our charge-spin order pattern matches closely the mechanism sketched in Fig.1b of Ref.[12]. Our result clearly agrees with magnetometry ruling out ferromagnetism and μSR ’s lower-bound moments $0.5 \mu_B$ as well as asymmetry lineshapes suggesting

long-range order [1].

The AFD structure, with in-plane couplings J_L and J_S (Fig.1), consists of two interpenetrating simple-cubic antiferromagnetic-G lattices (circles, dashed lines, and, respectively, squares and solid lines in Fig.1). The AFD magnetic energy does not depend on J_S , so the two sublattices are decoupled, and the critical temperature can be estimated for each separately. Since only the e_g orbitals parallel to the Ni-O bond are spin-polarized and contribute to the magnetic coupling, the diagonal J_S exchange interaction is arguably negligibly weak. From the energies of AFD and ferromagnetic (FM) phases, since $E_{\text{AFD}}-E_{\text{FM}}=(8J_L+4J_S) \mu_{\text{Ni}_{\text{II}}}^2 \simeq 8J_L \mu_{\text{Ni}_{\text{II}}}^2$ (Fig.1), we extract an antiferromagnetic $J_L=-5.6$ meV. The FM is also insulating and has the same moments, structure, and charge-ordering pattern, showing that the AFD ordering is simply driven by AF superexchange. As the vertical coupling J_\perp across the LAO layer should be very weak compared to the in-plane J_L (i.e. the anisotropy J_L/J_\perp is large), we identify the transition temperature with the Ne  l temperature of the 3D anisotropic AF Ising model [13] in the asymptotic large anisotropy limit: the result is $T_N \sim 35$ K, not far from the experimental 40 K. This comparison, of course, implies the assumption that above T_N the disordered spins fluctuate rapidly enough –say, frequency ≥ 1 MHz– so as not to be revealed by μSR .

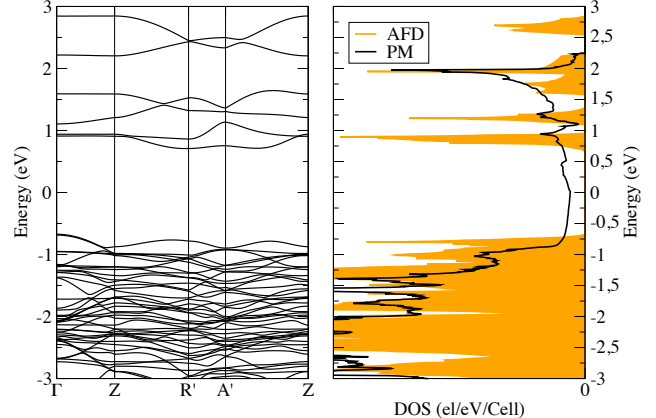


FIG. 2. (Color on line) Bands of the AFD phase (left) and total DOS of the AFD (orange, shaded) and Pauli-PM (solid line) states (right). Energy zero is the Fermi energy.

Electronic structure and metal-insulator transition – We now address electronic properties and discuss mechanisms of metal-insulator transition. Fig.2 reports the bands (left) and the total density of states (DOS) of AFD and of the Pauli-PM. The concurrent structural dimerization and magnetic superstructure open an (indirect) electronic gap of 1.3 eV in the AFD phase. The $\text{Ni}_{\text{IV}}\text{-}\text{Ni}_{\text{II}}$ charge transfer is associated in optical experiments to a spectral weight depletion below 0.4 eV, identified as a “charge gap” [1]. Our best shot at this result is the (indeed somewhat larger) electronic gap, originating from

the combined structure, charge and magnetic ordering.

The key point about the electronic structure is that the octahedra distortion is essential to obtain a gap. Forbidding distortion, all simulated phases are metallic and show no charge transfer. Only the Pauli-PM metal is stable among these (for example, the G-type AF dimerizes spontaneously to a ferrimagnetic marginal metal with Ni-Ni charge transfer). This suggests that the IMT be associated to the structural dimerization, and that the transition T_c be identified as that at which the structure un-dimerizes thermally, with attendant gap closure. Using a model analogous to molecular desorption dynamics, we describe the initially full population $N_0 \equiv N(t=0)$ of distorted structural units (contracted and expanded Ni-octahedron pairs) as undergoing thermal activation out of the low-T ground state. The population $N(t) = N_0 \exp(-Rt)$ is abruptly depleted, i.e. the system removes the distortion and hence the insulating character, whenever the Arrhenius activation rate $R = \nu_0 \exp(-\Delta E/k_B T)$ becomes appreciable (say, unity). Since the Pauli-PM is the only stable undimerized state, we envisage an AFD-PM transition and use the AFD-PM energy difference $\Delta E = 0.40$ eV per Ni pair. With a plausible effective vibrational prefactor $\nu_0 = 5$ THz [14], $R = 1$ Hz corresponds to $T_c \simeq 150$ K, in fair agreement with experiment.

Fermi surface – Confirming earlier theoretical suggestion [7, 11], the Pauli-PM phase has a single-sheet hole-like Fermi surface (Fig.3, left panel) centered at the 1×1 Brillouin zone corner, and analogous to optimally-doped cuprates, except for the states character being mixed e_g instead of pure x^2-y^2 . We also consider the un-dimerized AF-G phase: its Fermi surface, shown in Fig.3, right panel, recalls that of *underdoped* cuprates, with hole-like and electron-like pockets at the points known as nodal and antinodal in cuprates, which is not unexpected for that magnetic modulation [15].

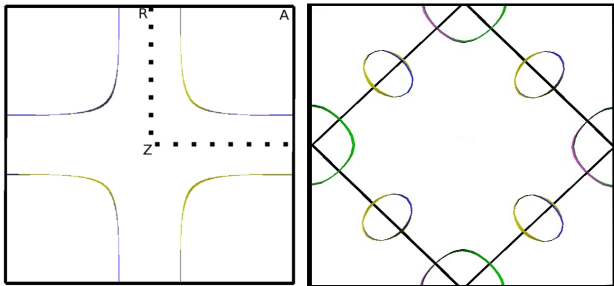


FIG. 3. (Color on line) Fermi surface of the Pauli-PM (left) and the AFD (right) phases in the 1×1 Brillouin zone.

The nearly two-dimensional pockets in Fig. 3 should give rise to quantum oscillation as function of inverse magnetic field. The frequency of about 20 kTesla for the PM might be observable (frequencies up to 30 kTesla were observed e.g. in indium [16]). The AF-G frequen-

cies are near those typical [15, 17] of underdoped cuprates (600 and 1800 Tesla for hole and electron pockets); however, their observability is barred by the AF-G state being unstable against dimerization and attendant onset of AFD magnetic order.

Transport – Since we cannot calculate the T dependence of dielectric response measured in [1], we use Bloch-Boltzmann theory to calculate the *dc* conductivity, with the goal of associating the transition T with the zero of $d\sigma/dT$, as suggested in [1]. We tune the energy dependence of the relaxation-time model [10] to reproduce the shape (not the value) of σ in the metal phase using the Pauli-PM bands. The model is then fed the AFD bands to produce the ground-state conductivity vs T.

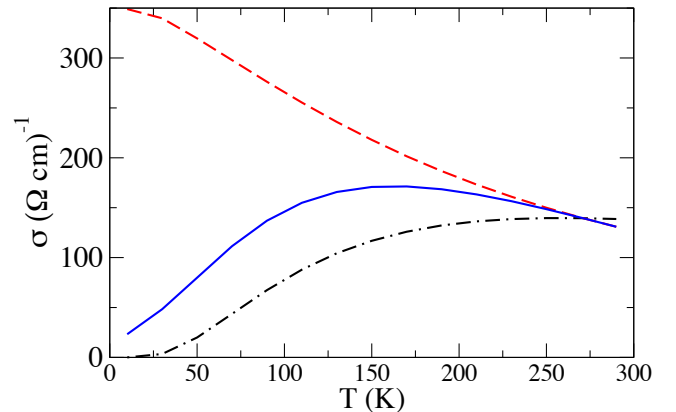


FIG. 4. Calculated conductivity vs. T for the metallic PM phase (dashed) and n -doped AFD phase (dash-dot); solid line: linear interpolation of the metal and insulator curves. The value of μ is fixed at the vertical dashed line in Fig.5.

We conjecture that the un-dimerization metal-insulator transition will cause the conductivity to cross over smoothly from the insulator to the metal. This can only be assessed qualitatively in the present context. First, our method cannot describe the “dirty” metal phase, which exhibits unusually low experimental conductivity; to account for this, we rescale the calculated metal σ by a factor 1/15, the ratio of the relaxation time [1] for the SL metal phase to that of a good metal (Al). Second, the insulating phase’s experimental conductivity is much higher than that of our undoped insulator at these temperatures. We obviate to this calculating the insulator σ for the chemical potential μ set to n -type, hence assuming implicitly a background doping of unidentified origin. In Fig.4 we interpolate linearly the two σ ’s just discussed (dashed and dash-dotted lines) vs.T, obtaining a result (solid line) qualitatively similar to experiment ([1], Fig. S8B of supporting material) and with $d\sigma/dT=0$ around 150 K, consistent with un-dimerization. We note in passing that $\log \sigma$ in the insulator phase is linear in $1/T$. Hopping behavior, as observed in [2], may be due to local disorder [18], which we cannot assess.

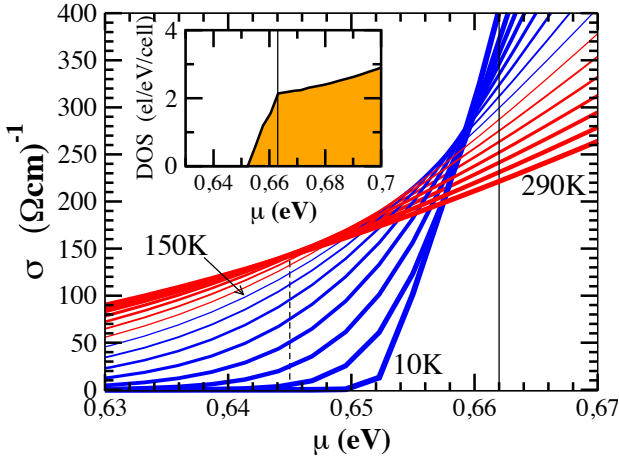


FIG. 5. (Color on line) Conductivity vs. chemical potential and T from 10 K, thickest blue (black) line to 290 K, thickest red (gray) line (20-K steps). Inset: DOS near conduction edge. Dashed (solid) vertical line marks intermediate regime (metallic crossover). Chemical potential zero at midgap.

Conductivity calculations for μ in n -type conditions suggest a further possible, concurrent transition mechanism. $\sigma(\mu, T)$ in Fig. 5 exhibits three regimes as function of μ . Initially, σ is insulator-like vs. μ and T, saturating at high T for fixed μ ; then, for μ just below the conduction edge, σ is insulator-like at low T, and crosses over at higher T to a normal-metal-like linear decrease; finally, at larger μ , σ decreases with T (and grows with μ) linearly as in a normal metal. This behavior is related to the slope change of the AFD near-conduction DOS (inset of Fig. 5), with the crossover to metallic conduction occurring for μ above the DOS cusp (vertical solid line). The insulator $\sigma(T)$ in Fig. 4 is obtained for μ just below the conduction edge (dashed vertical line in Fig. 5), and has $d\sigma/dT=0$ at about 250 K. This calculation thus shows that an insulator-metal crossover can also be legitimately associated to a conduction-band-edge Fermi level pinning (e.g. by shallow-donor defects). Clearly, this mechanism would be preempted by, or at most concurrent with, the un-dimerization transition discussed earlier, which is robustly rooted in the structural and magnetic energetics.

Summary – Ab initio calculations suggest that LNO/LAO ultra-short-period SLs have a structurally- and valency-dimerized charge-ordered insulator ground state, making distinct order-disorder and metal-insulator phase transitions at temperatures around 35 K and 150 K respectively to a metal phase with a cuprate-like Fermi surface. This interpretation is in good agreement with available experimental data.

We thank A. Boris for helpful discussions. Work supported in part by the EU via project OxIDES, by IIT via a Seed grant, by MIUR via project 2DEG-FOXI, and by Fondazione Banco di Sardegna grants. Computing re-

sources provided by CASPUR, CINECA, and Cybersar.

- [1] A. V. Boris, Y. Matiks, E. Benckiser, A. Frano, P. Popovich, V. Hinkov, P. Wochner, M. Castro-Colin, E. Detemple, V. K. Malik, C. Bernhard, T. Prokscha, A. Suter, Z. Salman, E. Morenzoni, G. Cristiani, H.-U. Habermeier, and B. Keimer, *Science* **332**, 937 (2011)
- [2] J. Liu, S. Okamoto, M. van Veenendaal, M. Kareev, B. Gray, P. Ryan, J. W. Freeland, and J. Chakhalian *Phys. Rev. B* **83**, 161102(R) (2011); J. Liu, M. Kareev, S. Prosandeev, B. Gray, P. Ryan, J. W. Freeland, and J. Chakhalian, *Appl. Phys. Lett.* **96**, 133111 (2010)
- [3] A. Filippetti and N. A. Spaldin, *Phys. Rev. B* **67**, 125109 (2003); A. Filippetti, C. D. Pemmaraju, S. Sanvito, P. Delugas, D. Puggioni, and V. Fiorentini, *Phys. Rev. B* **84**, 195127 (2011).
- [4] A. Filippetti and V. Fiorentini, *Eur. Phys. J. B* **71**, 139 (2009); T. Archer, C. D. Pemmaraju, S. Sanvito, C. Franchini, J. He, A. Filippetti, P. Delugas, D. Puggioni, V. Fiorentini, R. Tiwari, and P. Majumdar, *Phys. Rev. B* **84**, 115114 (2011).
- [5] M. J. Han and M. van Veenendaal, arXiv:1201.5369v1; A. Blanca-Romero and R. Pentcheva, *Phys. Rev. B* **84**, 195450 (2011); G. Giovannetti, private communication.
- [6] for example the Fermi surface in the PM phase is analogous to that in [7], and the pseudo-gapped density-of-states in metallic magnetic phases (results not discussed here) is similar to that of DMFT at large U [8].
- [7] P. Hansmann, X. Yang, A. Toschi, G. Khaliullin, O. K. Andersen, and K. Held, *Phys. Rev. Lett.* **103**, 016401 (2009).
- [8] P. Hansmann, A. Toschi, X. Yang, O. K. Andersen, and K. Held, *Phys. Rev. B* **82**, 235123 (2010).
- [9] V. Scagnoli, U. Staub, Y. Bodenthin, M. García-Fernández, A. M. Mulders, G. I. Meijer and G. Hammerl, *Phys. Rev. B* **77**, 115138 (2008).
- [10] A. Filippetti, P. Delugas, M. J. Verstraete, I. Pallecchi, A. Gadaleta, D. Marré, D. F. Li, S. Gariglio, and V. Fiorentini, to be published (2012).
- [11] J. Chaloupka and G. Khaliullin, *Phys. Rev. Lett.* **100**, 016404 (2008).
- [12] I. I. Mazin, D. I. Khomskii, R. Lengsdorf, J. A. Alonso, W. G. Marshall, R. M. Ibberson, A. Podlesnyak, M. J. Martínez-Lope, and M. M. Abd-Elmeguid, *Phys. Rev. Lett.* **98**, 176406 (2007).
- [13] M. Yurishchev, arXiv:cond-mat/0312555.
- [14] G. Gou, I. Grinberg, A. M. Rappe, and J. M. Rondinelli, *Phys. Rev. B* **84**, 144101 (2011).
- [15] A. Filippetti, D. Puggioni, and V. Fiorentini, *Europhys. Lett.* **88**, 67009 (2009).
- [16] J. H. P. van Weerent and J. R. Anderson, *J. Phys. F: Met. Phys.* **3**, 2109 (1973).
- [17] N. Doiron-Leyraud, C. Proust, D. LeBoeuf, J. Levallois, J.-B. Bonnemaison, X. Liang, D. A. Bonn, W. N. Hardy, and L. Taillefer, *Nature (London)* **447**, 565 (2007).
- [18] E. Detemple, Q. M. Ramasse, W. Sigle, G. Cristiani, H.-U. Habermeier, E. Benckiser, A. V. Boris, A. Frano, P. Wochner, M. Wu, B. Keimer, and P. A. van Aken, *Appl. Phys. Lett.* **99**, 211903 (2011).